From Semantic Segmentation to Semantic Registration: Derivative-Free Optimization-Based Approach for Automatic Generation of Semantically Rich As-Built Building Information Models from 3D Point Clouds

Fan Xue[1], Weisheng Lu[2], Ke Chen[3], and Anna Zetkulic[4]

This is the peer-reviewed, post-print version of the paper:

Xue, F., Lu, W., Chen, K., & Zetkulic, A. (2019). From semantic segmentation to semantic registration: Derivative-free optimization-based approach for automatic generation of semantically rich as-built building information models from 3D point clouds. *Journal of Computing in Civil Engineering*, 33(4): 04019024. Doi: 10.1061/(ASCE)CP.1943-5487.0000839

Highlights

- This paper proposes a new 'semantic registration' paradigm for reconstructing as-built BIMs from 3D point clouds.
- This paper develops a derivative-free optimization approach as well as a BIM software plugin to realize the 'semantic registration' paradigm.
- This paper employs two processes of surface sampling and voxelization for efficient estimation of geometric errors between a BIM and a point cloud in the derivative-free optimization approach.
- The effectiveness and the sensitivity of the approach was validated using a noisy indoor furniture case (100% precision and recall, RMSE=3.87cm, in 0.8s per BIM component), and the scalability was tested in a lecture hall case with 293 chairs (over 80% precision and recall, RMSE = 8.1cm, in about 5.0s per BIM component).
- The proposed 'semantic registration' paradigm is proven: (i) free from segmentation, (ii) capable of processing complex scenes, and (iii) reusing online open BIM resources.

[1] Research Assistant Professor, Department of Real Estate and Construction, The University of Hong Kong, Pokfulam, Hong Kong SAR, Email: xuef@hku.hk;

[2] Associate Professor, Corresponding Author, Department of Real Estate and Construction, The University of Hong Kong, Pokfulam, Hong Kong SAR, Email: wilsonlu@hku.hk;

[3] Postdoctoral Fellow, Department of Real Estate and Construction, The University of Hong Kong, Pokfulam, Hong Kong SAR, Email: leochen@connect.hku.hk;

[4] Senior Research Assistant, Department of Real Estate and Construction, The University of Hong Kong, Pokfulam, Hong Kong SAR, Email: zetkulic@hku.hk;

Abstract

Development of semantically rich as-built building information models (BIMs) presents an ongoing challenge for the global BIM and computing engineering communities. A plethora of approaches have been developed which, however, possess several common weaknesses: (1) heavy reliance on laborious manual or semi-automatic segmentation of raw data (e.g., 2D images or 3D point clouds); (2) unsatisfactory results for complex scenes (e.g., furniture or non-standard indoor settings); and (3) failure to use existing resources for modelling and semantic enrichment. This paper aims to advance a novel, derivative-free optimization (DFO)-based approach that can automatically generate semantically rich as-built BIMs of complex scenes from 3D point clouds. In layman's terms, the proposed approach recognizes candidate BIM components from 3D point clouds, reassembles the components into a BIM, and registers them with semantic information from credible sources. The approach was prototyped in Autodesk Revit and tested on a noisy point cloud of office furniture scanned via a Google Tango smartphone. The results revealed that the semantically rich as-built BIM was automatically and correctly generated with a root-mean-square error (RMSE) of 3.87 cm in a sheer 6.44 seconds, which outperformed the well-known Iterative Closest Point (ICP) algorithm. The approach was then scaled up to a large auditorium scene consisting of 293 chairs to generate a satisfactory output BIM with a precision of 81.9% and a recall of 80.5%. The 'semantic registration' approach also proved superior to existing 'segmentation approaches' in that it is segmentation-free, and capable of processing complex scenes and reusing known information. In addition to these methodological contributions, this approach, properly scaled up, will open new avenues for creation of building/ city information models from inexpensive data sources and support profound value-added applications such as smart building or smart city developments.

Keywords: Building information model (BIM); 'as-built' BIM; semantic enrichment; derivative-free optimization; semantic registration.

Introduction

A building information model (BIM) is a digital representation of the physical and functional characteristics of a facility and serves as a shared knowledge resource for decision-making throughout its lifecycle (NIBS, 2015). BIM has evolved from a buzzword into a technological hallmark of the architecture, engineering, construction, and operations (AECO) industry (Eastman et al., 2011; Xiong et al., 2013; Pătrăucean et al., 2015). Properly integrated with

geographic information systems (GIS) or city information models (CIM), it can mature into an indispensable component of urban-scale information infrastructure and enable various urbanization initiatives (Lu et al., 2018). The development of 'as-built' or 'as-is' BIMs is at the core of these potential applications.

An 'as-built' BIM is a representation of a facility as actually constructed or as it currently exists (Tang et al., 2010). Semantic information contained in a BIM generally consists of details specific to individual construction components (e.g., position, geometric size and shape, non-geometric type, material specification, and meanings of functions) and their relationships (e.g., dependency, topology, and joints) (e.g., Belsky et al., 2016). Some semantic information vital to a facility, such as *actual* building geometries, *current* functions, and *real* topology, can only embodied in as-built BIMs (Tang et al., 2010; Pătrăucean et al., 2015). In addition, the as-built condition of a facility will differ from when it was designed (i.e., an as-designed BIM) due to design changes, inadvertent deviations or errors, and renovation work. To better support new and complex applications, therefore, the AECO community continues to pursue the generation of semantically rich as-built BIMs.

A wealth of technological approaches has been developed to generate as-built BIMs. Volk et al. (2014) delineate these approaches as either data-driven or model-driven. A data-driven method performs modeling based on the extraction of features, shapes, materials, and statistics from the preprocessed measurement data, while a model-driven method generally refers to comparing the known components against the datasets (e.g., point clouds or imagery), recognizing components, and fitting them in a BIM based on pre-defined rules (Xue et al., 2018b). Manual creation of as-built BIMs by professional modelers is often adopted but this process is extremely tedious, time-consuming, and error-prone (Pătrăucean et al., 2015; Perez-Perez et al., 2016; Xue et al., 2018a; Tang et al., 2010; Jung et al., 2014), and these limitations become insurmountable when modeling at an urban scale (i.e., inputting BIM with CIM). For this reason, the prevailing research has focused on semi-automatic or fully automatic methods of as-built BIM generation.

Input measurement data for as-built BIM generation range from 2D imagery to point clouds. The latter, which can be collected using any type of 3D scanner, have become increasingly affordable and thus popular in recent years (Tang et al., 2010; Wang et al., 2017). Considerable advances have also been made in point cloud preparation and pre-processing proficiencies (e.g.,

Song et al., 2014; Zhang et al., 2016) in model generation methods (e.g., Bosché et al., 2015; Díaz-Vilariño et al., 2015) and for semantic enrichment (Belsky et al., 2016; Hamledari et al., 2017; Sacks et al., 2017). For example, by cloaking the geometry of an existing facility as meshes, a model can mimic the real-life object and its exterior and interior surfaces with millimeter accuracy. However, semantic information, such as functions, materials, volumes, and topology, continues to present an immense challenge in as-built BIM generation. Conventional approaches rely on 'semantic segmentation', which is a computer vision or graphics technology that assigns each 3D point, or 2D pixel, to one of several semantic labels (Shamir, 2008; Vezhnevets and Buhmann, 2010) via *a priori* rules-enabled reasoning models (e.g., Valero et al., 2012; Chen et al., 2018b), and training example-enabled machine learning models like deep learning (e.g., Babacan et al., 2017; Zou et al., 2017). Although these approaches have achieved acceptable results on simple and regularly shaped components such as walls, windows, pipelines, and boxes of internal walls (e.g., Valero et al., 2012; Babacan et al., 2017; Nguyen and Choi, 2018; Zou et al., 2018), they have yet to satisfactorily deal with complex scenes such as furniture, irregularly shaped components, and non-geometric information (e.g., Koppula et al., 2011; Wang et al., 2018).

This paper contends that the inadequacies of conventional semantic segmentation approaches are rooted in their methodology. The essence of semantic segmentation is to establish a correlation model between the input geometries and the output semantic labels, such as functions (e.g., OmniClass), materials, and invisible internal details (e.g., steel bars in a joint) (see Shamir, 2008; Vezhnevets and Buhmann, 2010; Koppula et al., 2011). The 'geometry-to-label' correlation models (i.e., *a priori* rules and trained machine learning models) are usually sound and clear for simple and regularly shaped components. The labeled points can further form 3D geometric primitives for volumetric objects (Martinovic et al., 2015; Zou et al., 2017; 2018). However, the segmentation of point clouds for uncontrolled real-world scenarios featuring heterogeneous components is fundamentally challenging due to too many labels, complex geometries, and complicated topologies (Andreopoulos and Tsotsos, 2013). In other words, the correlation models (*a priori* rules, geometric features, or machine learning techniques) are fundamentally constrained in labeling complex components.

There is also a missed opportunity from conventional methods, which disregard readily available resources that could facilitate semantic enrichment. Existing methods can only recognize limited semantics from the measurement data (e.g., 3D point clouds) concerning

geometric surfaces. However, information resources for 3D modeling and semantic enrichment already exist in the form of numerous public and private BIM databases, such as the National BIM Library (nationalbimlibrary.com; over 6,500 components), BIM Object (bimobject.com; over 290,000 components), those maintained by producers (e.g., steelcase.com), localized libraries (e.g., Lu et al., 2017), and private BIM databases actively maintained by developers and contractors (HKHA, 2010; Chen et al., 2017). All these are actually missed resources that could serve as credible BIM semantics sources for as-built BIM generation.

This paper reports a novel 'semantic registration' approach for automatic generation of semantically rich as-built BIMs from 3D point clouds. This approach fundamentally differs from existing semantic segmentation approaches in that it is segmentation free, capable of processing complex scenes, and able to cleverly reuse existing information. The theoretical stance of this approach is an extension of Xue et al. (2018a; 2018b), which formulate the task of generating as-built BIMs from a given measurement as a constraint optimization problem to reassemble candidate BIM components for the measurement. The remainder of this paper comprises five sections. The second section reviews the relevant research on as-built BIM generation and derivative-free optimization (DFO) applications in computing engineering. The third section presents the proposed approach. The fourth describes the experimental tests of the proposed approach in Autodesk Revit. Discussions concerning the advantages and shortcomings of the proposed approach appear in the fifth section, and the sixth recapitulates and concludes the study.

Literature review

Generation of as-built BIMs from 3D point clouds

The process involves first collecting and pre-processing a facility's actual conditions as point clouds. Numerous advanced non-contact sensing technologies are available for such data collection. One can capture the measurements of a facility on foot with a handheld *augmented reality* (AR) smartphone. For larger facilities, one can use a vehicle-borne *light detection and ranging* (LiDAR) scanner, a consumer *unmanned aerial vehicle* (UAV) or drone flown at low altitude, fixed-wing aircraft-borne LiDAR at a high altitude, or *interferometric synthetic aperture radar* (InSAR) at low Earth orbit (Tang et al., 2010; Zhu and Shahzad, 2014; Wang *et al*., 2017). If the directly measured data exists as multiple 2D images, *structure from motion* (SfM) or *simultaneous localization and mapping* (SLAM) can convert the images to 3D point clouds by estimating the camera positions and fusing with 3D scenes (Snavely et al., 2008).

Equally numerous are the data-driven or model-driven methods researchers have developed to generate as-built BIM from 3D point clouds (Shamir, 2008; Vezhnevets and Buhmann, 2010; Xiong et al, 2013). Nevertheless, these data-driven and model-driven types of approaches (Volk et al., 2014) both rely heavily on semantic segmentation requiring geometry-to-label correlation models (e.g., based on rules or machine learning models). Examples of rule-based models include *random sample consensus* (RANSAC) for planar components (Schnabel et al., 2007; Lagüela et al., 2013; Jung et al., 2014), parametric curved surface components (Dimitrov et al., 2016), geometric simplification such as voxelization (Aijazi et al., 2013; Zhu et al., 2017), and asserted simple geometry (e.g., indoor boundary and rooftop primitives) from intersection of planes (Valero et al., 2012; Chen et al., 2018b). Some approaches have employed machine learning techniques for more complicated correlation models, like *support vector machines* (SVM) (Adan and Huber, 2011; Koppula et al., 2011; Perez-Perez et al., 2016; Wang et al., 2017) or convolutional neural networks (Babacan et al., 2017). Features such as color from imagery (Quintana et al., 2018) and geometric metrics (e.g., key points) from computer vision (Chen et al., 2018a; Wang et al., 2018) have been applied to enhance the correlation models.

Nevertheless, the semantic segmentation methods are tedious, time-consuming, and in some cases inaccurate, especially for complex scenes. For example, Koppula et al.'s (2011) SVM model exhibited roughly 80% precision and 70% recall for office point clouds, but only roughly 50% precision and 50% recall for homes. The deep learning model in Babacan et al. (2017) succeeded in segmenting walls and floors with over 90% precision and 90% recall, but showed unsatisfactory results for beams (40% precision) and doors (55% recall). Wang et al.'s (2018) method was effective in segmenting chairs from dense point clouds (about 90% recall), but less effective on sparse and noisy data (about 40% recall). In summary, the semantic segmentation methods flounder when faced with the fundamental challenge of segmenting complex components. Uncontrolled real-life environments characterized by diversity of labels, irregular geometries, and topological relationships all make semantic segmentation even less satisfactory (Andreopoulos and Tsotsos, 2013).

Registration of credible, available BIM components is a possible means of responding to this difficulty. The concept of parametric 3D component registration emerged decades ago, for example in computer-aided design (CAD) surface fitting in reverse engineering (Varady et al.,

1997), and has been practiced in modeling curved surfaces (e.g., Dimitrov et al., 2016), pipelines (e.g., Bosché et al., 2014; Nguyen and Choi, 2018), secondary elements on walls (e.g., Adán et al., 2018), and historic BIMs (e.g., Barazzetti, 2016). A well-known registration algorithm is the iterated closest point (ICP). Kim et al. (2013) employed it to register an as-planned model to as-built point clouds. Sharif et al. (2017) used it to isolate the points of a complex BIM component and remove clutter points. A notable merit of this approach is its reuse of 3D geometry domain knowledge. Commercial software, e.g., IMAGINiT, PointFuse, Floored, and many in-house solutions were developed for supporting such generic registration approach. Yet, According to Bruno et al. (2018), there are only three technical papers on semi-automatic methods generating historic BIMs from point clouds and no paper on fully automatic methods. The reason was that the automatic registration of BIM components used to be confined by ineffective feature extraction and semantic segmentation (see Quattrini et al., 2015; Andreopoulos and Tsotsos, 2013). A recent breakthrough is the segmentation-free registration method in Xue et al. (2018a; 2018b), where the as-built BIM was generated by maximizing the *structural similarity* (SSIM) index between the input 2D images and the 2D projections of the BIM. Based on their problem formulation and semantic resources, complex components (e.g., furniture) became as easily recognizable as simple ones (e.g., walls). However, it is unclear whether the segmentation-free, 'semantic registration' approach (Xue et al., 2018a; 2018b) can be applied to 3D point clouds which, compared with 2D images, are generally noisier, bulkier, and less supported by scientific software libraries. It is thus the primary aim of this paper to advance a method that can automatically generate semantically rich as-built BIMs of complex scenes from 3D point clouds.

Derivative-free optimization and its applications

Registration of BIM components is often formulated as a mathematical function to optimize (e.g., Dimitrov et al., 2016; Xue et al., 2018a). The derivatives of a function universally contain vital information for finding its best values (i.e., minimum or maximum). However, in the problem of generating as-built BIMs from 3D point clouds the derivatives of objective functions are impractical to obtain (Rios and Sahinidis, 2013). Derivative-free optimization (DFO) is a class of nonlinear optimization that carries out optimization under such circumstances (Conn et al., 2009). Examples of DFO applications include *general pattern search* for protein structure prediction (Andreopoulos and Tsotsos, 2013) and surrogate management frameworks for optimization of cardiovascular geometries in surgical planning and treatment design (Marsden et al., 2008). CMA-ES (*covariance matrix adaptation evolution*

strategy) is another DFO algorithm that employs perturbations with expected values and an iteratively updated covariance matrix to guide the search for global optimization (Rios and Sahinidis, 2013); CMA-ES and its variants were proven among the most advanced algorithms for solving noisy problems (Hansen et al., 2010). In construction and civil engineering, Kaveh et al.'s (2011) applied CMA-ES for optimal design of a 26-story-tower space truss exhibited a 31% improvement in weight over a previous result by *genetic algorithm*, and Athanasiou et al.'s (2011) CMA-ES for structural system identification in earthquake engineering saw a 53% improvement from previous studies.

Xue et al. (2018b) applied the CMA-ES to as-built BIM generation and reconstructed an outdoor scene of a demolished building and an indoor furniture scene with a root-mean-square-error (RMSE) of 3.9 cm. However, several hours were spent generating the necessary small BIMs, which feature just a few components, the major issue being the thousands of model manipulations (e.g., creating, moving, rotating, scaling, and detecting components, while projecting 3D BIM to 2D images) on commercial BIM platforms. Thus, there remains room for improvement in efficiency of DFO algorithm application to as-built BIM generation. Another aim of this paper, therefore, is to make a contribution to this methodology.

The 'semantic registration' method for automatic BIM generation

Problem formulation

Essentially, the semantic registration method is to recognize candidate BIM components from 3D point clouds, reassemble the components into a BIM, and register them with semantic information from credible sources. In this formulation, the error between the as-built BIM and the input 3D point cloud is the objective function to minimize. Mathematical methods like DFO algorithms can automate the entire generation process. An overview of the formulation of the as-built BIM generation is shown in Figure 1. The two inputs of the proposed approach, as shown in Figure 1, are:

1) an input 3D point cloud P_{in} of m points ($\| P_{\text{in}} \| = m$) which represents the as-is conditions of a facility; and

2) a library of semantic BIM components (with both geometric and non-geometric semantic information) and topologies.

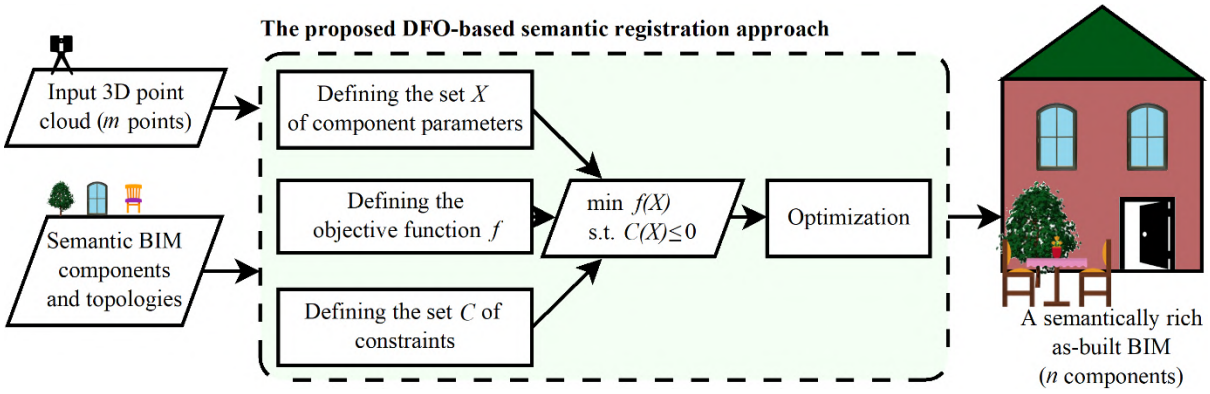

Figure 1. A conceptual framework of the proposed semantic registration approach

During the automatic as-built BIM generation process, some information, such as location, rotation, and topology, needs to be determined. This paper defines a tuple X of *variables* for each (e.g., i-th) component instance in the as-built BIM:

$$X_i = (cl, l, s, r), \tag{1}$$

where cl is the family class of the component (e.g., a meeting table), l is the 3D location, s is the 3D scaling, and r is the rotation which is usually around the z-axis (Note: some components such as a door handle may use other axes). The solving of X is equivalent to the object recognition in conventional segmentation-based methods. Other semantic information including surface texture, producer, and market price can be directly registered to the as-built BIM. Therefore, the output BIM is fully determined by $X = \{X_1, X_2, \ldots, X_n\}$, which represents a combination of all the parameters of n component instances, as shown in Figure 1. The candidate components and their topologies can be quickly filtered by scene (e.g., "indoor" and "office furniture") before problem-solving to reduce the computational load. The input 3D point cloud is the geometric reference frame for the as-built BIM.

The *objective function* f to minimize, in this paper, is the RMSE between the as-built BIM (determined by X) and the input 3D point cloud. The accurate RMSE can be calculated by computing the minimal distance to the as-built BIM *for each* point in the input cloud. However, since there can be a huge number of points in a cloud and another huge number of "faces" in an as-built BIM, the calculation of f is far too inefficient. In this paper, we first sample the surface of the BIM to a point cloud P_X with the same point density as the input cloud; so that the RMSE can be approximated by computing the RMSE between P_X and P_{in}, where $|P_X| \approx |P_{\text{in}}| = m$. Furthermore, we sample both point clouds by the voxelization method, which is proven effective for processing point clouds (Aijazi et al., 2013; Zhu et al., 2017), so that $|P'_X| \approx |P'_{\text{in}}|$

$= m' \ll m$. Advanced spatial data structures, such as oct-trees, can guarantee the RMSE computational time between P'_X and P'_{in} at $O(m' \log m')$ (Elseberg et al., 2013). Thus, we have the objective function f in Figure 1 defined and approximately simplified as:

$$
\begin{aligned}
f(X) &= RMSE(BIM(X), P_{\text{in}}) \\
&\approx RMSE(P_X, P_{\text{in}}) \qquad (2) \\
&\approx RMSE(P'_X, P'_{\text{in}}) = \sqrt{\Sigma_{p \in P'_{\text{in}}} nndist^2(p, P'_X)/m'} \\
&\approx RMSE(P'_{\text{in}}, P'_X) = \sqrt{\Sigma_{p \in P'_X} nndist^2(p, P'_{\text{in}})/\|P'_X\|} \\
&= f_{\text{X}}(X)
\end{aligned}
$$

where *BIM* is the surface of BIM determined by X, *nndist* is the Euclidean distance between a point and its nearest neighbor in another point cloud, and f_{X} is the approximate objective function. Eq. (2) implies that $f_{\text{X}}(X) \approx f(X)$, where the P'_X (down-sampled BIM surface) can be accumulated through model generation, so that it is not necessary to repeatedly calculate the whole BIM on commercial BIM platforms. As a result, the result of approximate objective (f_{X}) is very close to that of f, but f_{X} is much easier to calculate than f.

The variables X to optimize are constrained by possible domains, topological requirements, and conventions. An example of a topological requirement is that of a wheeled office chair sitting on a horizontal plane. An example of a convention is that of an office chair location likely to be next to a desk or table. Among the components, there exist a small group of topological relationships such as adjacency (e.g., *above*, *below*, and *next-to*), separation, containment, intersection, and connectivity (Nguyen et al., 2005). Thus, we can formulate the constraints C in Figure 1 as:

$$C(X) = \{C_{\text{I}}(X_i)\} \cup \{C_{\text{R}}(X_i, X_j), i \neq j\}, \qquad (3)$$

where C_{I} indicates the constraints on the parameters X_i of any i-th individual component, and C_{R} is the constraints on the topological relationships between any pair of (i-th, j-th) components. Examples of the two groups of constraints can be found in Table 1.

Table 1. Example of constraints in the proposed formulation

C	*Example*	*Example value*	*Notes*
C_I	*scaling_max*	[2.0, 2.0, 1.5]	*xyz* coordinates
	scaling_min	[0.5 0.5, 0.75]	*Ibid.*
	z_rotation_max	2π	
	z_rotation_min	0	
C_R	*on_top_of*	'Ground'	Adjacency, connectivity
	contains_on	'Wall'	Containment or intersection

After the formulation of the variables *X*, objective function *f*, and constraints *C*, we have a general form of the overall optimization problem of as-built BIM generation:

$$\begin{aligned} &\text{minimize} \quad f(X) = RMSE(BIM(X), P_{\text{in}}) \\ &\text{subject to} \quad C(X) \leq 0. \end{aligned} \tag{4}$$

Based on the popular optimization mechanisms in existing literature, Xue et al. (2018a) proposed a one-by-one, incremental generation process. In such a process, the problem-solving focuses on recognizing one component at a time and *n* incremental runs to complete the as-built BIM. An overall fine-tuning process of all the components after the incremental phase has also proven helpful in improving accuracy of the as-built BIM.

Problem solving

Based on the COBIMG, which stands for *constrained optimization-based BIM generator* (available at: https://github.com/ffxue/cobimg) software library (Xue et al., 2018b), the authors developed the "COBIMG-Revit", which is an automatic as-built BIM generation plugin for a popular BIM platform (i.e., Autodesk Revit). Figure 2 shows the three major modules of COBIMG-Revit. The first module, the core algorithm, is CMA-ES integrated in COBIMG. The second module is a new module, i.e., the *f*(*X*) calculation based on Eq. (2), where the functions of voxelization and *k*d-tree search are employed from PCL (point cloud library). The third module is the component assembly (e.g. creation, hiding, movement, rotation, and surface sampling of the as-built BIM) extended from COBIMG. The input components were a set of annotated Revit component families. The COBIMG-Revit, encapsulated as a plugin, interacts with Autodesk Revit via its C++ APIs and generates the as-built BIM in Revit project format.

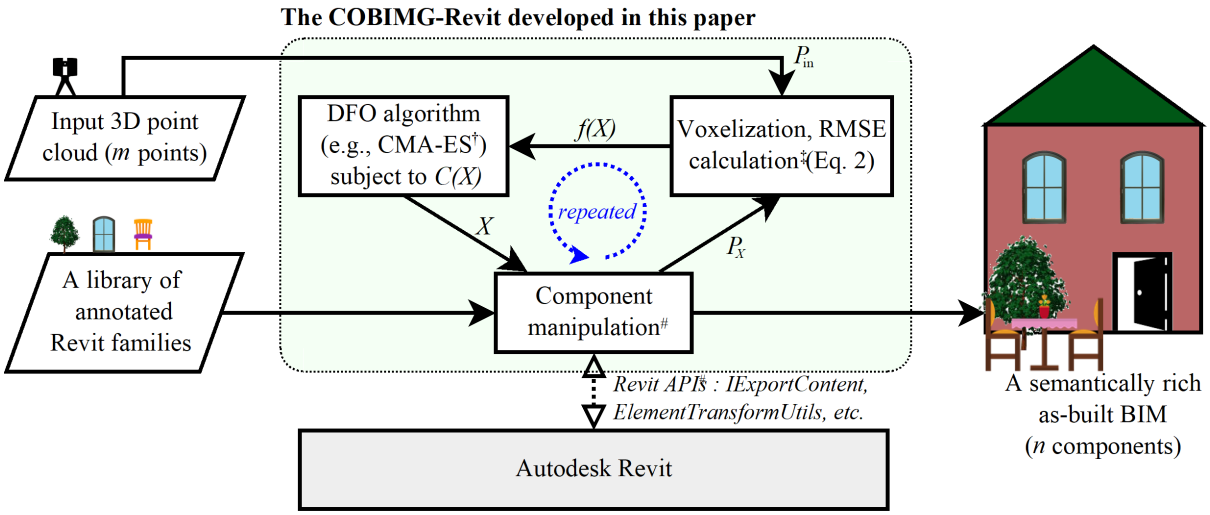

† : In C++, supported by libcmaes (version 0.9.5, available at: https://github.com/beniz/libcmaes)
‡ : In C++, supported by PCL (version 1.8.1, with FLANN, available at: http://pointclouds.org)
 # : In C++-compatible CLR, supported by Autodesk Revit (version 2015 Educational, documents at: http://www.revitapidocs.com)

Figure 2. Key modules, software libraries, and execution processes of COBIMG-Revit

Recognizing any i-th component is an automatic, iterative, trial-and-error procedure. As shown in Figure 3, the three modules of COBIMG-Revit operate in the same sequence for each trial. The trial starts from a feasible X_i that meets all the constraints. The component assembly module decodes the values of X_i to Revit family class (cl), location (l), scaling (s), and rotation (r). Then, the i-th component is modified (or created for the first trial) through Revit APIs based on the decoded parameters. The surface of the updated as-built BIM with the modified i-th component is sampled by the component assembly module to a point cloud P_X. The next module samples Pin and PX down with voxelization and returns the RMSE (i.e., $f(X_i)$), back to the first module of core algorithms. Finally, the core algorithm CMA-ES updates its covariance matrix and evolves its search strategy for succeeding trials.

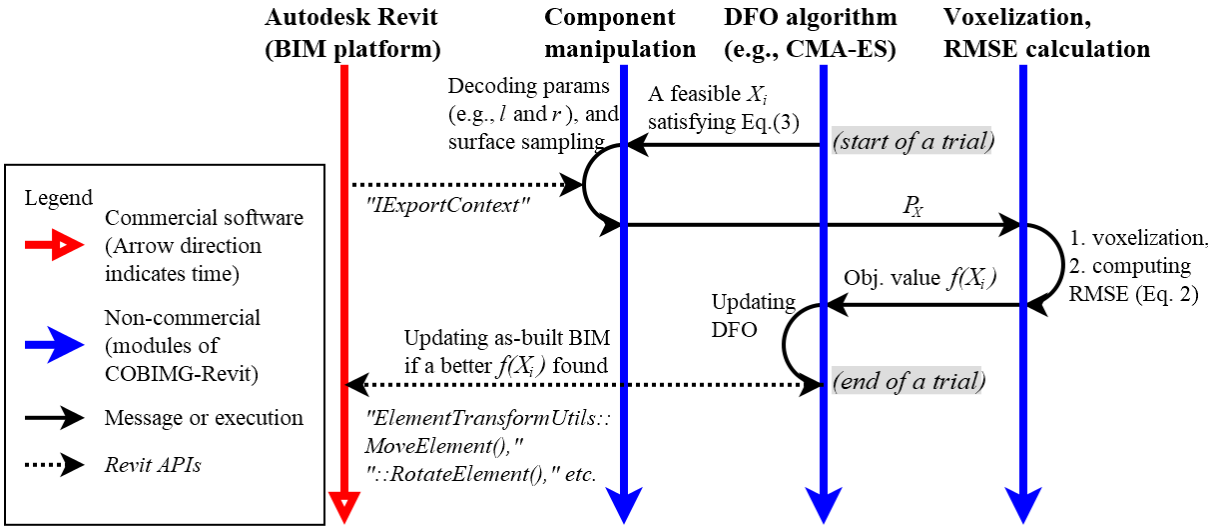

Figure 3. Message sequence chart of the operations and interactions between the modules of COBIMG-Revit in an individual trial

The incremental generation phase can be explained as follows. At the very beginning, the first component is always an invisible *Ground* component, or a similar fundamental component, which can be directly computed from the boundary of the input 3D point cloud. Therefore, during the whole incremental generation phase, there are $(i - 1)$ components already assembled before the i-th component. A "parent" component, either *Ground* or one of the assembled components, is sequentially selected to regulate a physical target area (e.g., a planar surface, a linear joint, or a room space) and a topological relationship (see Table 1) for the i-th component candidates to reside on. COBIMG-Revit then runs a few trials for each component candidate for the least RMSE. After trial-and-error tests on all the possible candidates, the component with the least RMSE is recognized as the i-th component in the as-built BIM. Meanwhile, the topological relationship between the i-th component and its parent is also confirmed. In such an incremental fashion, the whole BIM and its topology can be gradually built from the library of Revit families.

The nature of the incremental generation implies an asymmetric precedence of recognition of the n components in the as-built BIM. That is, the i-th component may influence the assembling of the j-th component only if $i < j$; but not vice versa. The asymmetric precedence thus may lead to a loss in accuracy of the as-built BIM. To complement the possible loss of accuracy, a fine-tuning phase runs after the incremental generation. In this phase, the parameters of each component, except for *Ground*, are re-optimized. If the re-optimization brings a better (i.e.,

less) RMSE, the BIM is changed based on the new parameters. The step-by-step fine-tuning continues until a terminate condition (e.g., a time limit) is met. The output as-built BIM is a project model (.rvt) in Revit.

Experiments

Experiment setting

An experiment was set to validate the proposed approach. The test case featured a noisy laboratory scene filled with furniture (see Figure 4), for which recognition proved challenging for traditional semantic segmentation approaches. The test scene consisted of two discussion tables, a round table, two footstools and three wheeled chairs, one with high armrests and two with low armrests. The 3D point cloud in Figure 4, with 194,813 points, was scanned by a Google Tango smartphone (Model: Lenovo PB2-690Y). The smartphone manipulated an infrared distance sensor and two cameras to estimate the indoor point cloud, which proved noisy, as shown in Figure 4. The scanning took about 20 minutes and the pre-processing (i.e., registration and stitching) roughly 15 minutes. There is no semantic segmentation in the experiments. The Revit families of the furniture, as listed in Table 2, were downloaded from the producer's website: steelcase.com. The research team spent about four minutes annotating the Revit family (.rfa) with the C_I and C_R listed in Table 1. Figure 5 shows the graphic user interface (GUI) of COBIMG-Revit encapsulated as a plugin of Autodesk Revit 2015 Educational 64-bit. The GUI of COBIMG-Revit consists of three parts: 1) an input point cloud, 2) a list of the Revit families (i.e. component candidates), 3) the as-built BIM generation panel.

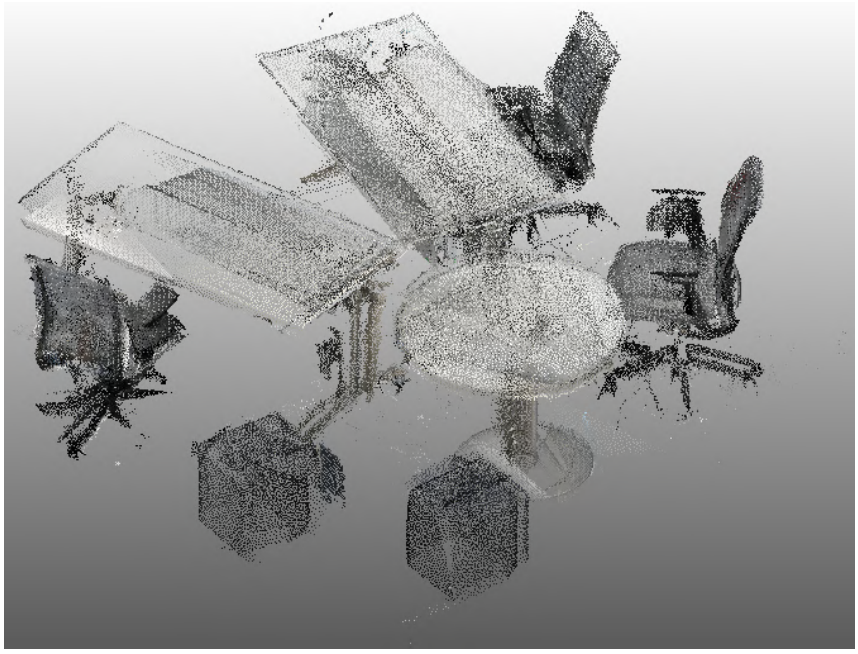

Figure 4. An indoor furniture scene with 194,813 noisy points scanned by a smartphone

Table 2. A list of the annotated semantic BIM components

Model of component	FlipTop Twin Table	Groupwork Coffee Table	Think V2 chair (high armrest)	Think V2 chair (low armrest)	B-Free footstool
3D view of component (screenshot in Revit)		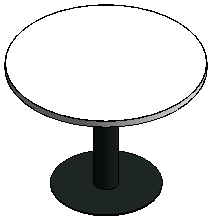			
C_I	s_{min}, s_{max}, r_{min}, and r_{max}				
C_R	*on_top_of* = *Ground*				
Semantics from family	OmniClass number, manufacturer, model, materials, style number, product, website, product line, release date, cost, assembly code, assembly description, etc.				

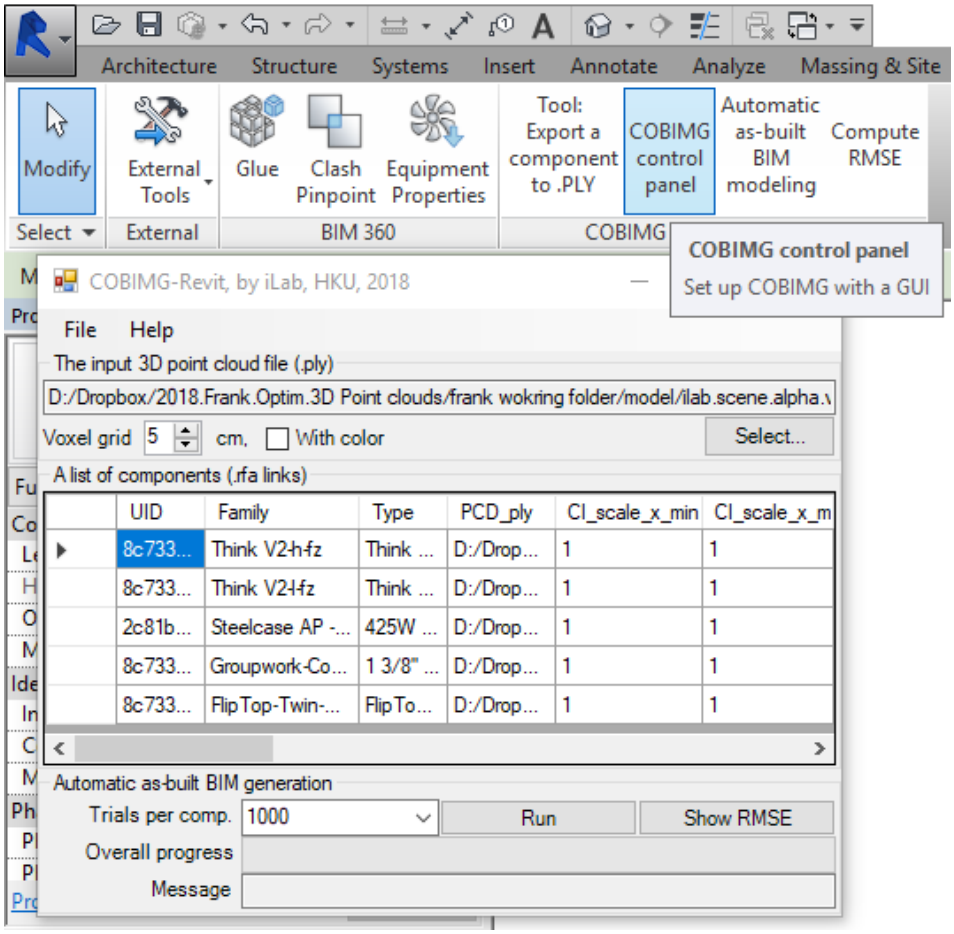

Figure 5. The user interface of COBIMG-Revit (on Revit 2015 Educational 64-bit)

The experiments were conducted at a workstation with two Intel XEON E5-2690 v4 CPUs (2.6GHz, 28 cores, 56 logical processors), 64 GB memory, and Windows 10 Enterprise 64-bit operating system. The invisible *Ground* was set to match the boundary of x and y of the input point cloud in Figure 4, with $z = 0$. The two major parameters of the proposed approach, as formulated in Sections 3.2 and 3.3, are the size of the voxel grid and the number of trials by CMA-ES per component (see the GUI in Figure 5). The size of the voxel grid was set in ten values from 1 cm to 10 cm in a linear order; while the number of trials was set in 10 values from 10 to 10,000 (10^4) in exponential order. COBIMG-Revit was also tested in a different number of threads to evaluate the acceleration by parallel computing. The team also tested the most popular point cloud registration algorithm ICP (see Kim et al. 2013; Sharif et al. 2017) for a comparison. We tested a number of variants of ICP, and selected one variant starting from random locations in parallel for a correct output. The number of the iterations of ICP was set to be equal to the number of trials of COBIMG-Revit.

Experimental results

The results of the experimental tests under different parameter settings, as shown in Figure 6, confirmed that the COBIMG-Revit was sensitive to the two parameters. Figure 6 shows three sets of experimental results (i.e., the number of correct components, the objective function, and the time cost in 56 threads) and a trade-off analysis from the tests under 100 configurations of the two parameters. Figure 6 (a) demonstrates that more trials generally led to more correct as-built BIMs when the grid size (i.e., resolution) was not too large (e.g., ≤ 8 cm); while in Figure 6 (b), f (RMSE) which was closely associated with correctness of components, showed a similar pattern. The trend on time cost in Figure 6 (c) shows that more trials and smaller grid size led to more computation time. The trade-off analysis in Figure 6 (d) shows that there exists an intersection of effectiveness (e.g., $f < 5$ cm, above the dashed polyline) and efficiency (e.g., < 10.5 s, below the curve of 10.5 s) for configuring the parameters. For instance, the research team selected a grid size of 5 cm and 500 trials for the test case.

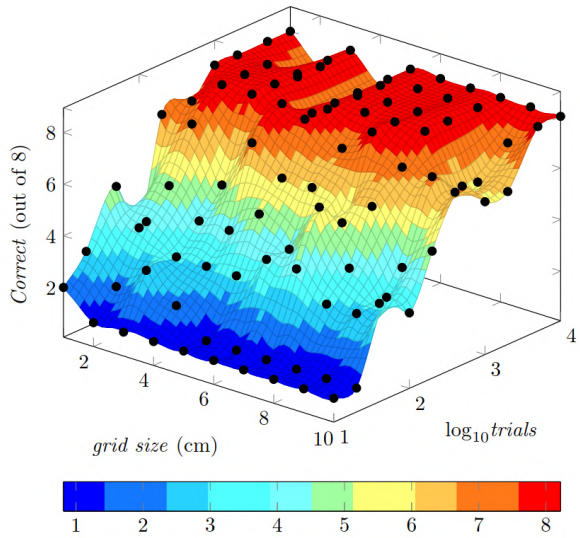

(a) The number of correct components (Note: higher is better)

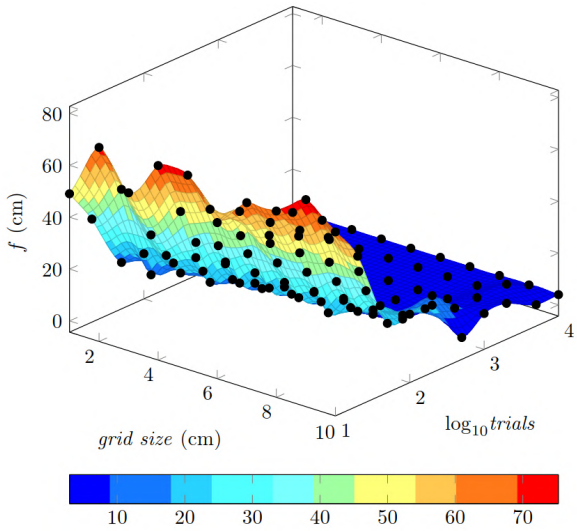

(b) The objective function (Note: lower is better)

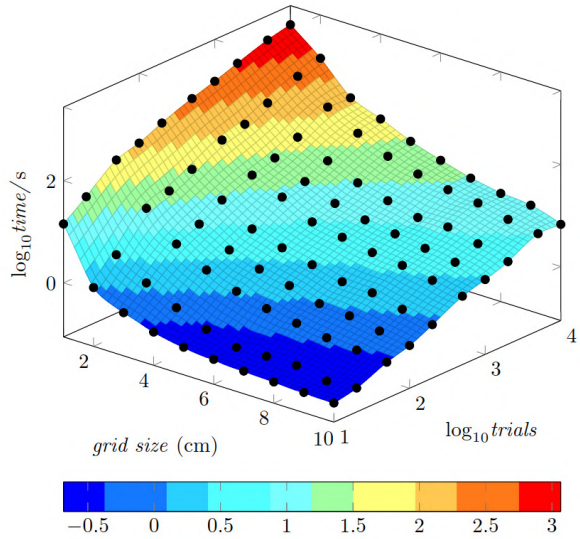

(c) The time cost (Note: in $\log_{10}$, i.e., lower is better)

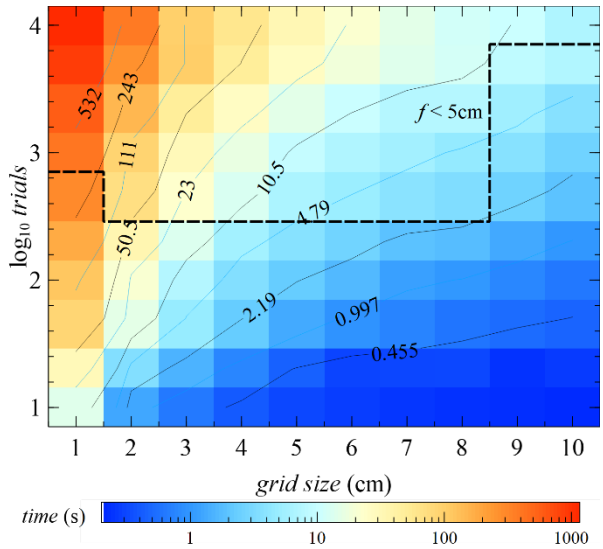

(d) A trade-off analysis

Figure 6. Experimental results of different parameter settings and a trade-off analysis on accuracy versus time cost of as-built BIM generation by COBIMG-Revit

Details of the problem-solving procedure by COBIMG-Revit are shown in Figure 7, with the selected grid size as 5 cm and 500 trials per component. The objective function f descended steadily from about 100 cm in the beginning when the as-built BIM was almost empty. When more and more components were incrementally added to the BIM, the two curves of f and f_X in Eq. (2), gradually approached one another; the convergence of the curves confirmed that the approximation in Eq. (2) is sound and effective. The incremental generation phase ended in 3.09 seconds after searching for the 9-th component in vain (no component had sufficient support of points). The result of the incremental generation phase was a BIM with 8

components on the *Ground* (f = 4.26 cm). The fine-tuning phase further improved the objective function down to f = 3.87 cm in 3.36 seconds by slightly changing the positions and rotations of the components, while the overall topology and the big picture of the as-built BIM remained the same. The overall time amounted to a sheer 6.44 seconds, and the output as-built BIM was saved as a Revit project (see Figure 8 (a)). A visual comparison in Figure 8 (b) shows that the output as-built BIM well matched the input 3D point cloud. In addition, the ground truth 3D presentations offered by the producer overcame to a considerable extent the noise present in the input, as shown in Figure 8 (b). In contrast, Figure 8 (c) shows the BIM generated by the ICP algorithm in 30.1s. There were five correct components and four wrong furniture as highlighted in Figure 8 (c). It can be seen that one FlipTop Twin table was mistakenly modeled as two Groupwork Coffee tables; the other fault was the two chairs with low armrests were registered as those with high armrests. Figure 8 (d) shows a top view of the point cloud and the BIM by ICP. The RMSE in Figure 8 (d) was 4.76 cm. In summary, the proposed COBIMG-Revit outperformed the well-known ICP algorithm in terms of correctness, geometric accuracy, and time cost.

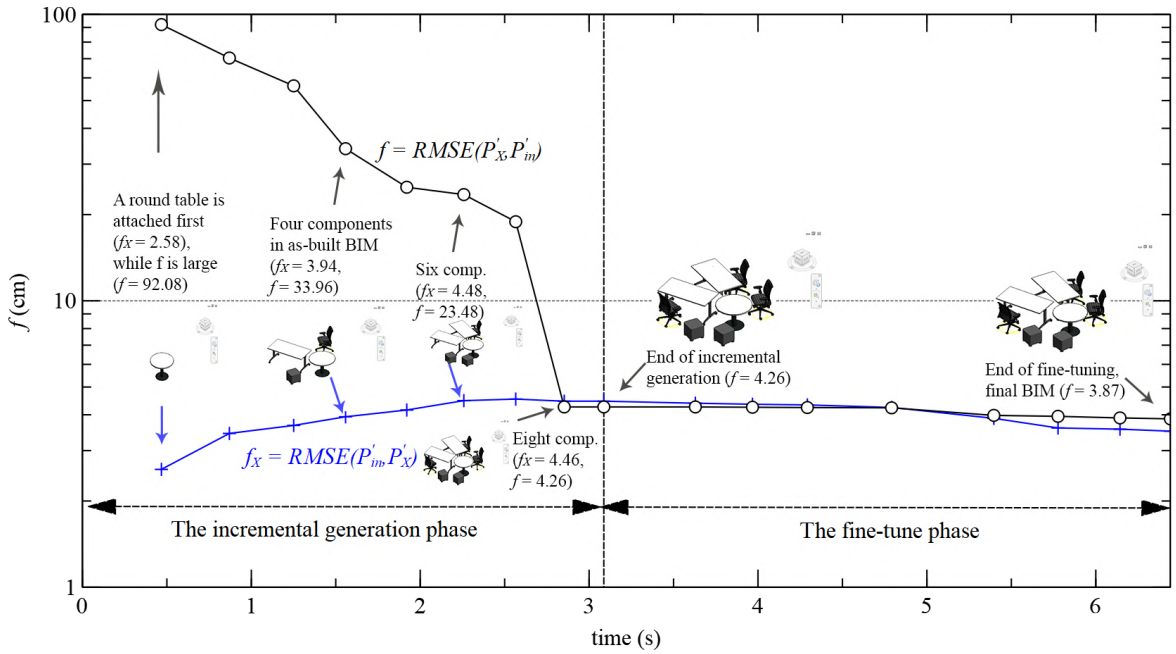

Figure 7. A typical problem-solving process of COBIMG-Revit (Parameters: grid size = 5 cm, 500 trials per component)

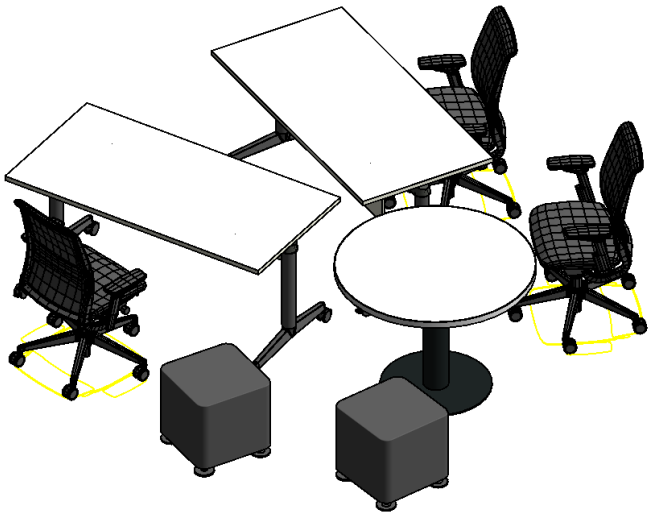

(a) A screenshot of the 3D view of the output as-built BIM

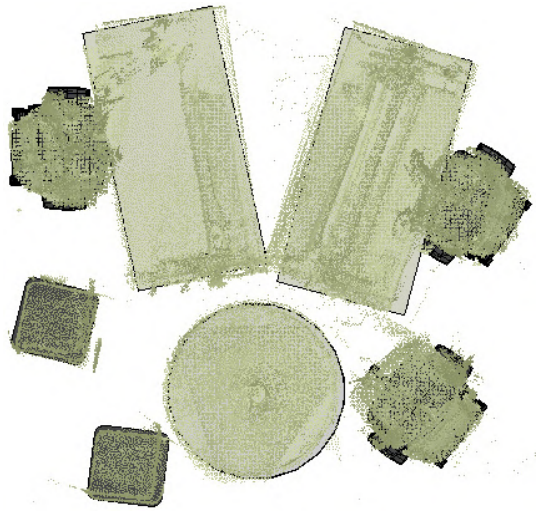

(b) A visual comparison between the input (grey points) and the output BIM

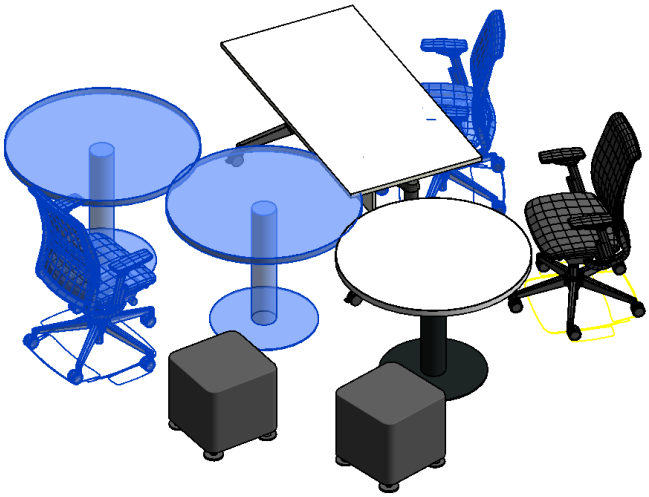

(c) A screenshot of the BIM generated by ICP (time = 30.1s, consisting of 4 wrong furniture)

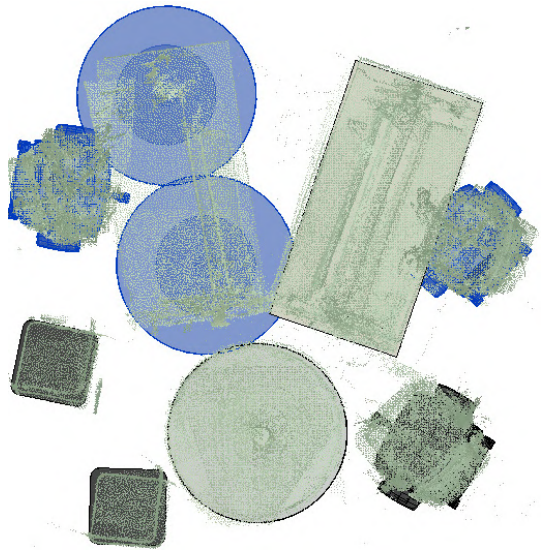

(d) A visual comparison between the input (grey points) and the BIM generated by ICP (RMSE = 4.76 cm)

Figure 8. Comparison of the generated as-built BIMs by COBIMG-Revit and ICP (Note: grid size = 5 cm, 500 trials per component, the wrong components are highlighted in blue)

The COBIMG-Revit then registered semantic information into the as-built BIM shown in Figure 8 (a). Figure 9 illustrates the properties of a *B-Free* footstool in the as-built BIM. The left window in Figure 9 shows the footstool's properties, including "COBIMG_translation", "COBIMG_rotation", and topological relationships (e.g., "COBIMG_parent"). The right window in Figure 9 shows the 'type' properties that contain the semantic information registered from the producer's online library (e.g., manufacturer, model, materials, style number, product

line, release date, assembly code, and assembly description). In fact, most of the registered properties were almost impossible to segment using the conventional approaches relying on rule-based and machine learning-based correlation models.

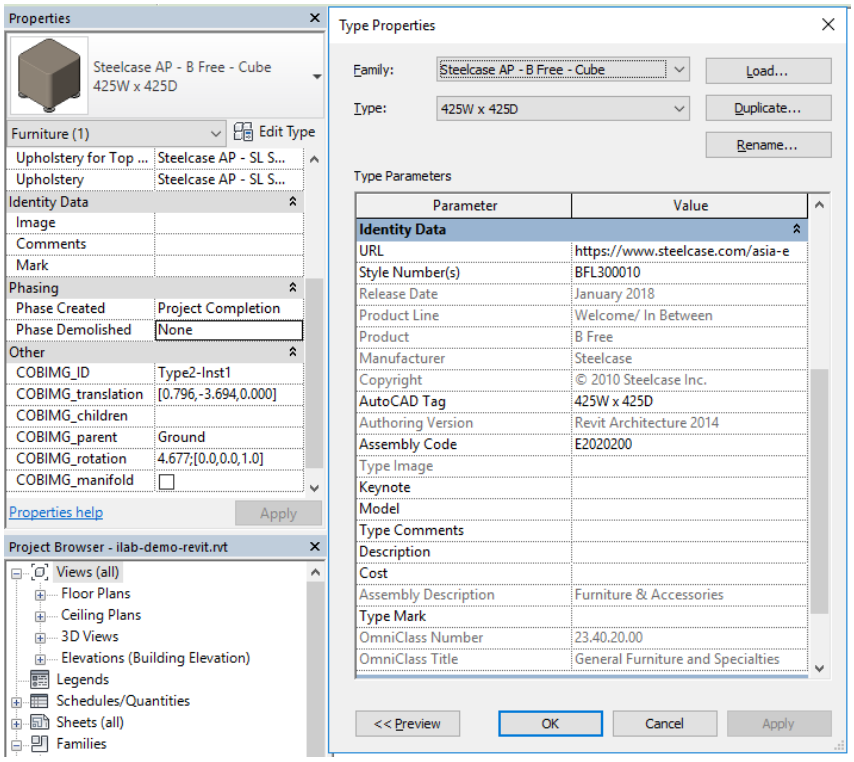

Figure 9. A screenshot of the semantic information in the as-built BIM

Parameters analysis

The team applied Pearson's bivariate correlation tests to evaluate the sensitivity of the two parameters of COBIMG-Revit (see Figure 6). Table 3 lists the results on the number of correct components, *f*, and time cost computed by IBM SPSS (version 24.0). It shows that the voxel grid size prompts a strong negative correlation to computation time (i.e., the greater the grid size, the less computation time), and no significant correlation to the number of correct components or *f*. In comparison, the number of trials has significant correlations with all three indicators (i.e., a very strong positive correlation with the correct components, a very strong negative correlation with *f*, and a strong positive correlation with the time cost). The analytical results suggest: 1) the voxelization can efficiently reduce the time cost without significant loss of accuracy in *f* (and a decrease in the number of correct components); 2) the number of trials per component should be large enough (e.g., 500 or above) for accurate as-built BIM generation.

Table 3. Pearson's correlations between the two parameters and the three algorithmic performance indicators (N = 100)

		No. of correct components	f (cm)	Time cost (s, in $\log_{10}$)
Grid size (cm)	Pearson cor.	-0.111	0.109	-0.656**
	Sig. (2-tailed)	0.270	0.282	0.000
No. of trials per component (in $\log_{10}$)	Pearson cor.	0.904**	-0.823**	0.690**
	Sig. (2-tailed)	0.000	0.000	0.000

**: Correlation is significant at 0.001 level (2-tailed).

The number of threads were also tested to evaluate the acceleration from multi-threading parallel computing. As shown in Figure 10, the overall time cost decreased, almost log-linearly, from about 70 seconds to 8 seconds while the number of threads increased from 1 to 14 (i.e., the number of the physical cores in one test CPU). There was a slight increase in time when the number of threads went beyond a single CPU due to the operational system (e.g., the load balancing of multiple CPUs). On two CPUs (i.e., with more than 14 threads), the time cost decreased log-linearly again. The curve in Figure 10 confirmed that COBIMG-Revit can make good use of the parallel computing hardware acceleration from everyday computers to high-end enterprise workstations.

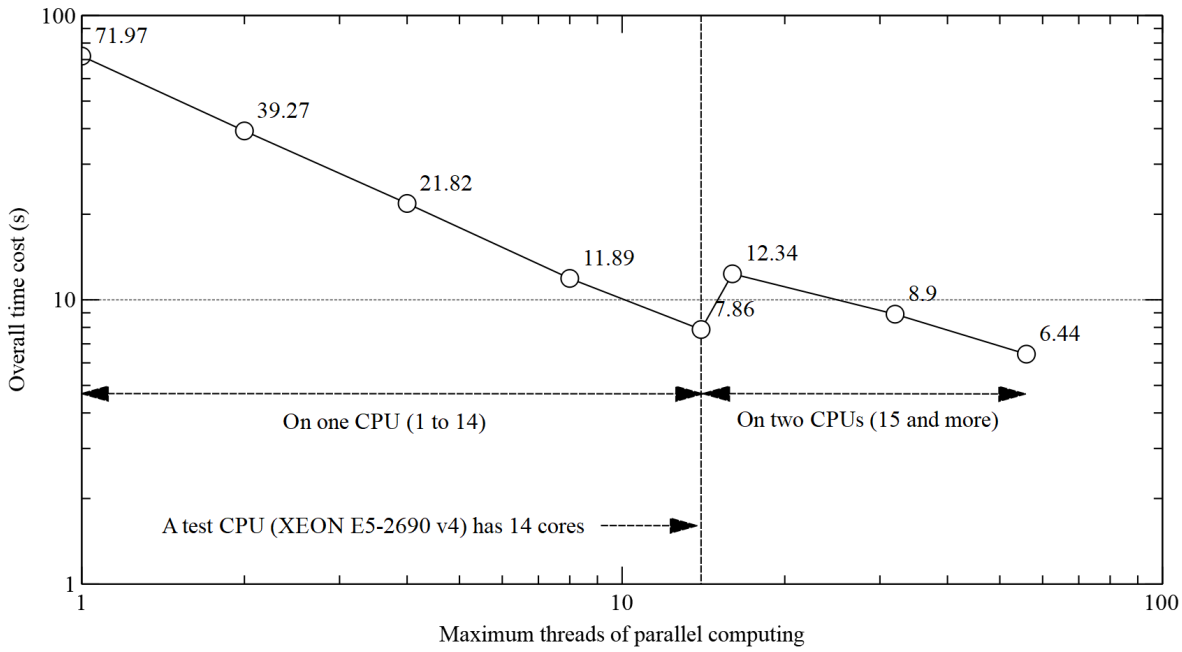

Figure 10. The computation time of COBIMG-Revit by multi-threading parallel computing

A comparison with manual modeling

The rationale of the semantic registration approach resembles closely the 'logo-stacking' style of a manual as-built modeling process. To compare accuracy and efficiency of the two approaches, the team invited three volunteer modelers with divergent levels of experience in Autodesk Revit to undertake manual modeling tests. The input 3D point cloud and the Revit family types were preloaded in the BIM software, and each modeler was required to select and adjust the furniture components to their correct locations (x and y) and rotations (around z), while the furniture components were placed on the default floor (z = 0) automatically in Revit. The modelers received a three-minute training course before they began. Table 4 lists the correctness, RMSE, and time cost of the three manually made as-built BIMs. In accuracy, COBIMG-Revit's output model ranked second after the model developed by the most experienced modeler. The modeling speed of COBIMG-Revit, however, was about 50 times that of the modelers. Although ICP was also faster than manual modelers, it failed to generate an accurate and correct BIM. COBIMG-Revit, as an automate approach, thus successfully addresses the challenges of manual modelling (e.g. tedium, slowness, and inaccuracy).

Table 4. The results of three manual as-built BIM generations, where the best value in each column is in bold

Modeler No.	Experience	Correctness (out of 8)	RMSE (cm)	Time cost (s)
1	Expert (3 years)	**8**	**3.79**	363.9
2	Average (1 year)	**8**	3.90	335.4
3	Beginner	**8**	4.22	691.1
COBIMG-Revit		**8**	3.87	**6.44**
ICP		5	4.76	30.1

Scalability tests

To test the scalability of the proposed approach, a cloud (about 1.9 million points) of 293 auditorium chairs, as shown in Figure 11 (a), from the Stanford 2D-3D-S dataset (Armeni et al., 2017) was selected according to the segmentation predefined in the dataset. Unlike the completeness in the office scene, there existed a low level of occlusion and clutters in the auditorium scene. There is no semantic segmentation in the experiments, either. As shown in Figure 11 (b), the ground at the rear area was about 1.0m higher than that in the front. Two

BIM components, 'Theater Chair' and 'Fixed Chair', were downloaded from 3DWarehouse.com, and then annotated. Apart from the topological relationship settings in Table 1, the translation over *z*-axis (l_z) was allowed from 0m to 1.0m in the annotation. The grid size of COBIMG-Revit was 5 cm; the number of trials was set to 5,000 due to an extra freedom on the *z*-axis; the multi-threading parallel computing was enabled. Each component was tested in an independent experiment because all the chairs were known identical.

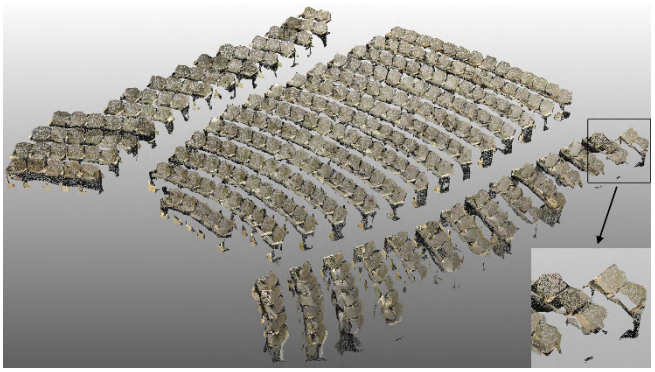

(a) A cloud of 1,879,282 points of chairs in the "Area_2 Auditorium_2" instance in the Stanford 2D-3D-S dataset (the zoomed area shows the occlusion and clutters)

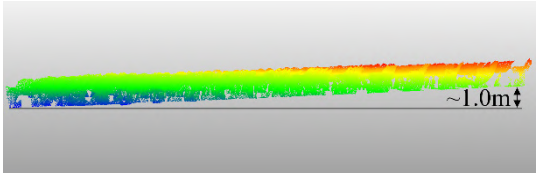

(b) The height ramp of the point cloud (i.e., rear chairs are about 1.0m higher)

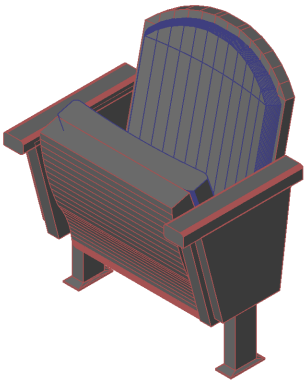

(c) 'Theater Chair' (author: AJ)

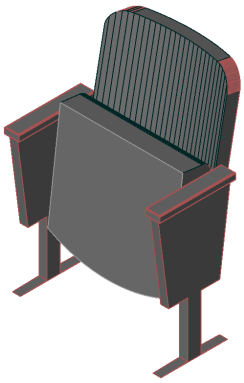

(d) 'Fixed Chair' (author: Veronica S.)

Figure 11. An auditorium scene of 293 identical theater chairs and two chair components

The COBIMG-Revit generated an output BIM as shown in Figures 12 (a) and (b) using the 'Theater Chair' component. As listed in Table 5, the output BIM consisted of 288 chairs, with an RMSE = 8.10 cm, and was saved as a 1.83 MB Revit project file. The other BIM, as shown in Figures 12 (c) and (d), were generated using the 'Fixed Chair' component with an RMSE = 9.15 cm. Figures 12 (b) and (d) show the comparisons with the input point cloud from the top view, where the major part of the input was correctly registered to chairs in both BIMs, the

false positive (with wrong location or rotation) chairs are highlighted, and the false negative (undetected) chairs are in circles. It can be found from Table 5 that the output BIM resembled the furniture setup of the auditorium scene using different components. The latter BIM had better precision and recall, but the first BIM had smaller RMSE, geometric error, and angular error. According to the objective function, e.g., Eq. (2), the BIM in Figure 12 (a) was selected as the output BIM from the noisy input.

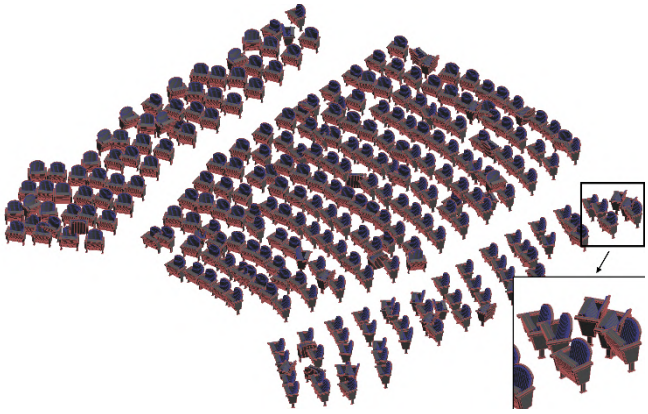

(a) Screenshot of the BIM consisting of 288 'Theater Chairs' (RMSE = 8.10cm, time =1,434.2s)

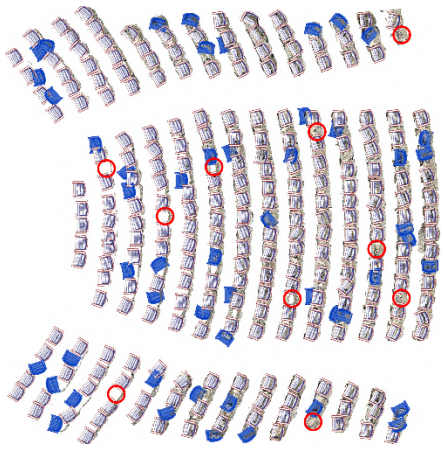

(b) Top view of (a) (false positive highlighted, false negative in circles)

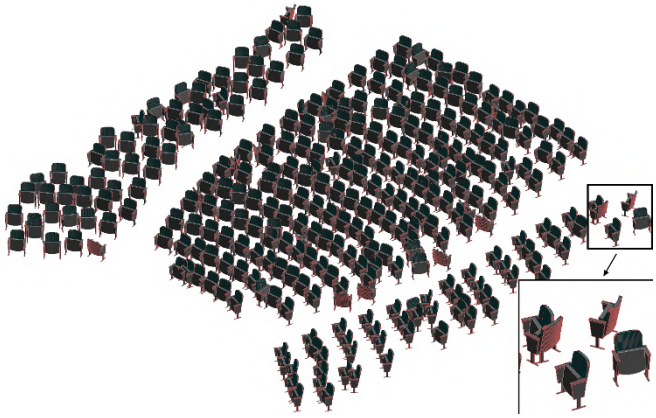

(c) Screenshot of the second BIM consisting of 312 'Fixed Chairs' (RMSE = 9.15cm, time = 1,538.3s)

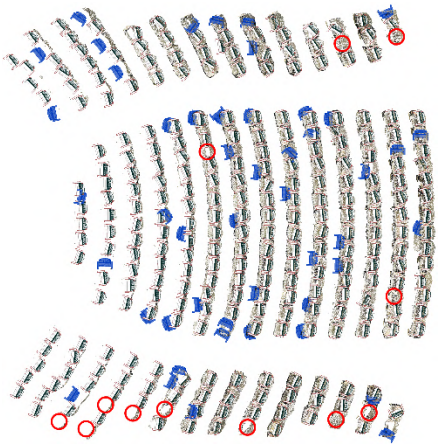

(d) Top view of (c) (false positive highlighted, false negative in circles)

Figure 12. Comparison of the BIMs using the 'Theater Chair' and another BIM using 'Fixed Chair'

Table 5. Comparison of the auditorium BIM generation using different component (better value in each row in bold)

Evaluation		'Theater Chair'	'Fixed Chair'
Time (s)		**1,434.2**	1,538.3
RMSE (cm)		**8.10**	9.15
Number of chairs		**288**	312
Output file size (MB)		**1.83**	2.19
Centroid distance error (cm)	Mean	**15.2**	15.8
	Std. dev.	**7.7**	8.6
Angular error (°)	Mean	**17.6**	19.7
	Std. dev.	**28.8**	34.6
Precision (%)		81.9	**84.3**
Recall (%)		80.5	**89.8**
F_1 (%)		81.2	**87.0**

Table 6 lists the detailed confusion matrix of the chairs in the two output BIMs in Figure 12. The metrics of the first output BIM can be calculated by:

$$\begin{aligned} &\textit{Precision} = \text{True positive / Number of chairs in BIM} = 236 / 288 = 81.9\% \\ &\textit{Recall} = \text{True positive / Ground truth number of chairs} = 236 / 293 = 80.5\% \\ &F_1 = 2 \times \textit{Precision} \times \textit{Recall} / (\textit{precision} + \textit{Recall}) = 81.2\% \end{aligned} \tag{5}$$

In Figure 12 and Table 6, there were 36 chairs generated in wrong positions, 16 chairs in correct positions but wrong directions. One reason of the incorrect positive is the exclusion of using repeated patterns of the chairs (e.g., Wang et al. 2018), while another is the noise in the input point cloud leading to the errors, as shown in the zoomed box in Figure 11 (a). The average time for generating a chair was about 5.0 seconds, considerably increased from the less than 1 second in the indoor office scene due to the increased number of trials. Overall, the satisfactory results of the test and the inexpensive computational time validate that the proposed 'semantic registration' approach is scalable to large-scale point clouds. Thanks to the embedded knowledge in the BIM components and the advanced DFO algorithms, the output BIM also outperformed many conventional semantic segmentation methods, e.g., Armeni et al. (2017), to achieve a 16.5% precision in the point-level – rather than the component level in this paper – classification of chairs.

Table 6. A confusion matrix of the generated chairs in the generated BIM by COBIMG-Revit

Evaluation	'Theater Chair'		'Fixed Chair'	
	Chairs	Not a chair	Chairs	Not a chair
Positive position and rotation	236	10	263	12
Positive position but negative rotation (error > 45°)	16	-	13	-
Negative position (error > 25cm*)	36	-	36	-
Subtotal	288	10	312	12

*: 25cm is a quarter of the diagonal of the target chair

Discussion

In contrast to conventional approaches dependent on semantic segmentation, the presented approach offers several advantages:

1) Complex building components can be accurately modeled via 3D point clouds, even atop noisy point clouds. In addition, the noise in the input point cloud considerably improves with the ground truth 3D presentations, as a part of the geometric semantics, from credible sources like the producer's library. Accuracy of the model generated using the proposed approach was close to that of manual models.

2) The proposed approach can be applied to simple and regularly shaped components. Although the efficiency may not be comparable with conventional segmentation approaches, it can include any pre-defined BIM components in Eq. (2).

3) The whole as-built BIM generation process is fully automatic. In conventional approaches, human modelers are still required to post-process the segmentation results (e.g., Jung et al., 2014).

4) Rich semantic information can be registered from credible semantic resources to produce a semantically rich as-built BIM. Computer programs can reuse semantic information from existing BIM resources for value-added applications.

5) Preparation of geometry-to-label correlation models, such as retrieval of rules from experts and collection of training examples for machine learning techniques, is not needed. Instead, credible and available BIM resources represent the domain knowledge for as-built BIM generation in the proposed approach.

6) The proposed approach boasts a high level of efficiency. By harnessing the power of parallel computing, such an efficient approach could promote wider use of as-built BIM within the AECO industry and inspire assorted smart city applications.

Despite its many merits, the proposed approach also has its shortcomings:

1) The proposed approach relies on structured BIM knowledge such as external sources, the geometric details, and the embedded semantics of BIM components and annotated topological requirements. For example, oversimplified BIM components (e.g., a box model of wheeled chair) that considerably changes the 5-cm sampled surface points may lead to inaccuracy in geometry and incorrect BIMs.

2) If the two mechanisms (i.e., surface sampling and voxel-based down-sampling) are not configured correctly, the fidelity of the output as-built BIM can be undermined, as shown in Figures 6 (a) and (b). A trade-off exists between speed and accuracy in as-built BIM generation, as shown in Figure 6 (d).

3) Although similar BIM components can come close to an approximated BIM (see Figures 11 and 12), the approach may not work on unique and tailor-made components due to its reliance on availability of BIM components. The approach may not work on scenes under heavy occlusion and distortion due to the unavailable geometric data.

4) The approach is yet to make good use of the 'instance parameters' in prevailing BIM software (e.g., Revit) to determine more accurate semantics such as the exact height of the armrest and its family class, location, and rotation.

5) The approach is yet to utilize 3D point color and texture information to determine more accurate semantics. It should also be noted that the infrared and laser scanned 3D point clouds usually do not represent reflective surfaces such as glass and waterbody; thus the surfaces with materials of glass and water in the components should be separated in the sampling process of the approach.

6) The overall computational time of the presented approach, as formulated in Section 3.2, grows at least in a linear relation to the number n of components.

7) The experiments in this paper are for a relatively complex scene but it needs to be scaled up in future studies, e.g., including all the building elements such as walls, floors, and columns as well as the possible patterns of their formations.

Conclusion

This paper presents a DFO-based 'semantic registration' approach for automatic generation of semantically rich as-built BIMs from 3D point clouds. This approach builds upon previous DFO-based approaches by exploiting 3D point clouds in prevailing BIM platform Revit, and by polishing the algorithms behind the application. The task of generating as-built BIMs is formulated to a constrained optimization problem by minimizing the error between the output BIM and the input 3D point clouds. The formulated problem is simplified by sampling the BIM surface and voxelization of the point clouds, and a well-known DFO algorithm, CMA-ES, is applied to solve the formulated and simplified problem. The BIM resulting from experiments on a noisy point cloud of an indoor furniture scene was accurate (RMSE = 3.87 cm), efficient (time = 6.44 s), and consisted of rich semantic information (e.g., materials, product line, and assembly code) registered from the manufacturer's library. The approach was also proved scalable for modeling large-scale point clouds.

This paper offers a trifold contribution to the BIM and computing engineering communities. It presents the first semantic registration approach for as-built BIM generation from 3D point clouds. Unlike the a *priori* rules or machine learning methods of predominant semantic segmentation schemes, the presented approach exploits available, credible semantic BIM resources to handle simple to complex scenes. Secondly, the presented DFO-based semantic registration approach is highly accurate and efficient in processing noisy complex point clouds and reusing public and private BIM resources. This paper also improves upon Xue et al.'s (2018a; 2018b) methodology (e.g., the time length of the experiment dramatically dropped from a few hours to a few seconds). In summary, the semantic registration approach presented here is superior to existing segmentation approaches in several ways: it is segmentation free, capable of processing complex scenes, and able to cleverly apply existing information for 3D modeling and semantic enrichment.

The innovative approach reported in this paper opens new avenues for professionals in the built environment and development field. Architects and designers, construction crews and engineers, facilities managers and conservationists can contribute to the realization of truly smart cities. It offers global business leaders and developers a more expedient and quality tool for creating semantically rich BIMs/CIMs. The proposed approach suggests that inexpensive data sources can be effectively and efficiently exploited to produce models of complex scenes and is a potential game-changer in the competitive landscape of BIM/CIM. The research team

recommends further studies follow to examine the applicability of the approach to other scenes, and its applicability on a wider, possible urban scale.

Acknowledgements

This study was supported by a grant from the Hong Kong Research Grant Council (GRF HKU17201717) and two grants from The University of Hong Kong (201702159013, 201711159016). We would like to thank the reviewers for their insightful comments and suggestions on improving the quality of the paper.

References

Adan, A. & Huber, D. (2011), 3D reconstruction of interior wall surfaces under occlusion and clutter. In 2011 International Conference on 3D Imaging, Modeling, Processing, Visualization and Transmission (3DIMPVT 2011), 275-281, Hangzhou, China. doi:10.1109/3DIMPVT.2011.42

Adán, A., Quintana, B., Prieto, S. A., & Bosché, F. (2018). Scan-to-BIM for 'secondary' building components. Advanced Engineering Informatics, 37, 119-138.

Aijazi, A. K., Checchin, P., & Trassoudaine, L. (2013). Segmentation based classification of 3D urban point clouds: A super-voxel based approach with evaluation. Remote Sensing, 5(4), 1624-1650.

Andreopoulos, A., & Tsotsos, J. K. (2013). 50 years of object recognition: Directions forward. Computer Vision and Image Understanding, 117(8), 827-891.

Armeni, I., Sax, S., Zamir, A. R., & Savarese, S. (2017). Joint 2D-3D-semantic data for indoor scene understanding. arXiv preprint arXiv:1702.01105.

Athanasiou, A., De Felice, M., Oliveto, G. & Oliveto, P. S. (2011). Evolutionary algorithms for the identification of structural systems in earthquake engineering. In Proceedings of the International Conference on Evolutionary Computation Theory and Applications - Volume 1: ECTA, (IJCCI 2011), 52-62. doi:10.5220/0003672900520062

Babacan, K., Chen, L. & Sohn, G. (2017). Semantic Segmentation of Indoor Point Clouds Using Convolutional Neural Network. ISPRS Annals of Photogrammetry, Remote Sensing and Spatial Information Sciences, IV-4/W4, 101-108.

Barazzetti, L. (2016). Parametric as-built model generation of complex shapes from point clouds. Advanced Engineering Informatics, 30(3), 298-311.

Belsky, M., Sacks, R., & Brilakis, I. (2016). Semantic enrichment for building information modeling. Computer-Aided Civil and Infrastructure Engineering, 31(4), 261-274.

Bosché, F., Ahmed, M., Turkan, Y., Haas, C. T. & Haas, R. (2015), The value of integrating Scan-to-BIM and Scan-vs-BIM techniques for construction monitoring using laser scanning and BIM: The case of cylindrical MEP components. Automation in Construction, 49, 201-213.

Bosché, F., Guillemet, A., Turkan, Y., Haas, C. T., & Haas, R. (2014). Tracking the built status of MEP works: Assessing the value of a Scan-vs-BIM system. Journal of Computing in Civil Engineering, 28(4), 05014004.

Bruno, S., De Fino, M., & Fatiguso, F. (2018). Historic Building Information Modelling: performance assessment for diagnosis-aided information modelling and management. Automation in Construction, 86, 256-276.

Chen, J., Fang, Y., & Cho, Y. K. (2018a). Performance evaluation of 3D descriptors for object recognition in construction applications. Automation in Construction, 86, 44-52.

Chen, K., Lu, W., Wang, H., Niu, Y., & Huang, G. G. (2017). Naming objects in BIM: A convention and a semiautomatic approach. Journal of Construction Engineering and Management, 143(7), 06017001.

Chen, K., Lu, W., Xue, F., Tang, P., & Li, L. H. (2018b). Automatic building information model reconstruction in high-density urban areas: Augmenting multi-source data with architectural knowledge. Automation in Construction, 93(9), 22-34..

Conn, A. R., Scheinberg, K., & Vicente, L. N. (2009). Introduction to derivative-free optimization (MPS-SIAM series on optimization), vol. 8, Philadelphia, PA, USA: SIAM.

Díaz-Vilariño, L., Conde, B., Lagüela, S. & Lorenzo, H. (2015), Automatic detection and segmentation of columns in as-built buildings from point clouds. Remote Sensing, 7(11), 15651-15667.

Dimitrov, A., Gu, R. & Golparvar-Fard, M. (2016), Non-uniform B-spline surface fitting from unordered 3D point clouds for as-built modeling. Computer-Aided Civil and Infrastructure Engineering, 31(7), 483-498.

Eastman, C. M., Eastman, C., Teicholz, P., & Sacks, R. (2011). BIM handbook: A guide to building information modeling for owners, managers, designers, engineers and contractors, 2nd Edition. John Wiley & Sons, Hoboken, New Jersey, USA.

Elseberg, J., Borrmann, D., & Nüchter, A. (2013). One billion points in the cloud–an octree for efficient processing of 3D laser scans. ISPRS Journal of Photogrammetry and Remote Sensing, 76, 76-88.

Hamledari, H., Rezazadeh Azar, E. & McCabe, B. (2017). IFC-based development of as-built and as-is BIMs using construction and facility inspection data: Site-to-BIM data transfer automation. Journal of Computing in Civil Engineering, 32(2), 04017075.

Hansen, N., Auger, A., Ros, R., Finck, S. & Pošík, P. (2010). Comparing results of 31 algorithms from the black-box optimization benchmarking BBOB-2009. In Proceedings of the 12th Annual Conference Companion on Genetic and Evolutionary Computation, 1689-1696. doi:10.1145/1830761.1830790

HKHA (Hong Kong Housing Authority) (2010). Building Information Modelling (BIM) Library Components Reference. Hong Kong.

Jung, J., Hong, S., Jeong, S., Kim, S., Cho, H., Hong, S., & Heo, J. (2014). Productive modeling for development of as-built BIM of existing indoor structures. Automation in Construction, 42, 68-77.

Kaveh, A., Kalateh-Ahani, M. & Masoudi, M. S. (2011). The CMA evolution strategy based size optimization of truss structures. International Journal of Optimization in Civil Engineering, 1(2), 233-56.

Kim, C., Son, H., & Kim, C. (2013). Automated construction progress measurement using a 4D building information model and 3D data. Automation in Construction, 31, 75-82.

Koppula, H. S., Anand, A., Joachims, T. & Saxena, A. (2011). Semantic labeling of 3D point clouds for indoor scenes. In Advances in Neural Information Processing Systems 24, 244-252. Available at: http://papers.nips.cc/paper/4226-semantic-labeling-of-3d-point-clouds-for-indoor-scenes.pdf

Lagüela, S., Díaz-Vilariño, L., Martínez, J. & Armesto, J. (2013). Automatic thermographic and RGB texture of as-built BIM for energy rehabilitation purposes. Automation in Construction, 31, 230-240.

Lu, W., Chen, K., Wang, J., & Xue, F. (2017). Developing an open access BIM objects library: A Hong Kong study. In Lean and Computing in Construction Congress-Volume 1: Proceedings of the Joint Conference on Computing in Construction. Heriot-Watt University. doi:10.24928/JC3-2017/0254

Lu, W., Peng, Y., Xue, F., Chen, K., Niu, Y., & Chen, X. (2018). The fusion of GIS and Building Information Modeling for big data analytics in managing development sites, in Comprehensive Geographic Information Systems, Elsevier, 345-359. doi:10.1016/B978-0-12-409548-9.09677-9

Marsden, A. L., Feinstein, J. A., & Taylor, C. A. (2008). A computational framework for derivative-free optimization of cardiovascular geometries. Computer Methods in Applied Mechanics and Engineering, 197(21-24), 1890-1905.

Martinovic, A., Knopp, J., Riemenschneider, H., & Van Gool, L. (2015). 3D all the way: Semantic segmentation of urban scenes from start to end in 3D. In the 2015 IEEE Conference on Computer Vision and Pattern Recognition (CVPR 2015), 4456-4465. Boston, MA, USA. doi: 10.1109/CVPR.2015.7299075

National Institute of Building Sciences (NIBS). (2015). National Building Information Modeling Standard. Version 3, Retrieved from https://www.nationalbimstandard.org/

Nguyen, C. H. P., & Choi, Y. (2018). Comparison of point cloud data and 3D CAD data for on-site dimensional inspection of industrial plant piping systems. Automation in Construction, 91, 44-52.

Nguyen, T. H., Oloufa, A. A. & Nassar, K. (2005). Algorithms for automated deduction of topological information. Automation in Construction, 14, 59-70.

Nicosia, G. & Stracquadanio, G. (2008). Generalized pattern search algorithm for peptide structure prediction. Biophysical Journal, 95(10), 4988-4999.

Pătrăucean, V., Armeni, I., Nahangi, M., Yeung, J., Brilakis, I. & Haas, C. (2015). State of research in automatic as-built modelling. Advanced Engineering Informatics, 29(2), 162-171.

Perez-Perez, Y., Golparvar-Fard, M. & El-Rayes, K. (2016). Semantic and geometric labeling for enhanced 3D point cloud segmentation. In Proceedings of Construction Research Congress 2016, 2542-2552. doi:10.1061/9780784479827.253

Quattrini, R., Malinverni, E. S., Clini, P., Nespeca, R., & Orlietti, E. (2015). From TLS to HBIM. High quality semantically-aware 3D modeling of complex architecture. International Archives of the Photogrammetry, Remote Sensing & Spatial Information Sciences, XL-5/W4, 367-374. doi: 10.5194/isprsarchives-XL-5-W4-367-2015.

Quintana, B., Prieto, S. A., Adán, A. & Bosché, F. (2018). Door detection in 3D coloured point clouds of indoor environments. Automation in Construction, 85, 146-166.

Rios, L. M., & Sahinidis, N. V. (2013). Derivative-free optimization: a review of algorithms and comparison of software implementations. Journal of Global Optimization, 56(3), 1247-1293.

Sacks, R., Ma, L., Yosef, R., Borrmann, A., Daum, S. & Kattel, U. (2017). Semantic enrichment for building information modeling: Procedure for compiling inference rules

and operators for complex geometry. Journal of Computing in Civil Engineering, 31(6), 04017062.

Schnabel, R., Wahl, R. & Klein, R. (2007), Efficient RANSAC for point-cloud shape detection. Computer Graphics Forum, 26(2), 214-226. doi:10.1111/j.1467-8659.2007.01016.x

Shamir, A. (2008). A survey on mesh segmentation techniques. Computer Graphics Forum, 27(6), 1539-1556

Sharif, M. M., Nahangi, M., Haas, C., & West, J. (2017). Automated Model-Based Finding of 3D Objects in Cluttered Construction Point Cloud Models. Computer-Aided Civil and Infrastructure Engineering, 32(11), 893-908.

Snavely, N., Seitz, S. M. & Szeliski, R. (2008). Modeling the world from internet photo collections. International Journal of Computer Vision, 80(2), 189-210.

Song, M., Shen, Z. & Tang, P. (2014), Data quality-oriented 3D laser scan planning. In Proceedings of Construction Research Congress 2014, 984-993. doi:10.1061/9780784413517.101

Tang, P., Huber, D., Akinci, B., Lipman, R. & Lytle, A. (2010). Automatic reconstruction of as-built building information models from laser-scanned point clouds: A review of related techniques. Automation in Construction, 19(7), 829-843.

Valero, E., Adán, A. & Cerrada, C. (2012). Automatic method for building indoor boundary models from dense point clouds collected by laser scanners. Sensors, 12(12), 16099-16115.

Varady, T., Martin, R. R., & Cox, J. (1997). Reverse engineering of geometric models—an introduction. Computer-Aided Design, 29(4), 255-268.

Vezhnevets, A., & Buhmann, J. M. (2010). Towards weakly supervised semantic segmentation by means of multiple instance and multitask learning. In 2010 IEEE Conference on Computer Vision and Pattern Recognition (CVPR 2010), 3249-3256, San Francisco, CA, USA. doi:10.1109/CVPR.2010.5540060

Volk, R., Stengel, J., & Schultmann, F. (2014). Building Information Modeling (BIM) for existing buildings—Literature review and future needs. Automation in Construction, 38, 109-127.

Wang, J., Wu, Q., Remil, O., Yi, C., Guo, Y., & Wei, M. (2018). Modeling indoor scenes with repetitions from 3D raw point data. Computer-Aided Design, 94, 1-15.

Wang, Q., Cheng, J. C. & Sohn, H. (2017). Automated estimation of reinforced precast concrete rebar positions using colored laser scan data. Computer-Aided Civil and Infrastructure Engineering, 32, 787-802.

Xiong, X., Adan, A., Akinci, B., & Huber, D. (2013). Automatic creation of semantically rich 3D building models from laser scanner data. Automation in Construction, 31, 325-337.

Xue, F., Chen, K., Liu, D., Niu, Y., & Lu, W. S. (2018a). An optimization-based semantic building model generation method with a pilot case of a demolished construction. In Proceedings of the 21st International Symposium on Advancement of Construction Management and Real Estate, 231-241. Springer, Singapore. doi:10.1007/978-981-10-6190-5_22

Xue, F., Lu, W., & Chen, K. (2018b). Automatic generation of semantically rich as-built building information models using 2D images: A derivative-free optimization approach. Computer-Aided Civil and Infrastructure Engineering, In Press. doi: 10.1111/mice.12378

Zhang, C., Kalasapudi, V. S. & Tang, P. (2016). Rapid data quality oriented laser scan planning for dynamic construction environments. Advanced Engineering Informatics, 30(2), 218-232.

Zhu, Q., Li, Y., Hu, H., & Wu, B. (2017). Robust point cloud classification based on multi-level semantic relationships for urban scenes. ISPRS Journal of Photogrammetry and Remote Sensing, 129, 86-102.

Zhu, X. X. & Shahzad, M. (2014). Facade reconstruction using multiview spaceborne TomoSAR point clouds. IEEE Transactions on Geoscience and Remote Sensing, 52(6), 3541-3552.

Zou, C., Colburn, A., Shan, Q., & Hoiem, D. (2018). LayoutNet: Reconstructing the 3D Room Layout from a Single RGB Image. In the 2018 IEEE Conference on Computer Vision and Pattern Recognition (CVPR 2018), 2051-2059. Salt Lake City, USA. In press.

Zou, C., Yumer, E., Yang, J., Ceylan, D., & Hoiem, D. (2017). 3D-PRNN: Generating shape primitives with recurrent neural networks. In 2017 IEEE International Conference on Computer Vision (ICCV), 2, 900-909. Venice, Italy. doi: 10.1109/ICCV.2017.103